Monitoring ligand–receptor interactions by photonic force microscopy

2010 Nanotechnology 21 255102

(http://iopscience.iop.org/0957-4484/21/25/255102)

Nanotechnology **21** (2010) 255102 (8pp) doi:10.1088/0957-4484/21/25/255102

Monitoring ligand–receptor interactions by photonic force microscopy

Sylvia Jeney[1,2], Flavio Mor[2], Roland Koszali[3], László Forró[2] and Vincent T Moy[4]

[1] M E Müller Institute for Structural Biology, Biozentrum, University of Basel, Klingelbergstrasse 70, Basel, 4056, Switzerland
[2] Laboratory of Complex Matter Physics (LPMC), Ecole Polytechnique Fédérale de Lausanne (EPFL), CH-1015 Lausanne, Switzerland
[3] Institute for Information and Communication Technologies (IICT), University of Applied Sciences of Western Switzerland (HEIG-VD), Rue Galilée 15, CH 1401 Yverdon-les-bains, Switzerland
[4] Department of Physiology and Biophysics, University of Miami Miller School of Medicine, 1600 NW 10th Avenue, Miami, FL 33136, USA

E-mail: sylvia.jeney@unibas.ch and vmoy@miami.edu

Received 6 February 2010, in final form 16 April 2010
Published 2 June 2010
Online at stacks.iop.org/Nano/21/255102

Abstract
We introduce a method for the acquisition of single molecule force measurements of ligand–receptor interactions using the photonic force microscope (PFM). Biotin-functionalized beads, manipulated with an optical trap, and a streptavidin-functionalized coverslip were used to measure the effect of different pulling forces on the lifetime of individual streptavidin–biotin complexes. By optimizing the design of the optical trap and selection of the appropriate bead size, pulling forces in excess of 50 pN were achieved. Based on the amplitude of three-dimensional (3D) thermal position fluctuations of the attached bead, we were able to select for a bead–coverslip interaction that was mediated by a single streptavidin–biotin complex. Moreover, the developed experimental system was greatly accelerated by automation of data acquisition and analysis. In force-dependent kinetic measurements carried out between streptavidin and biotin, we observed that the streptavidin–biotin complex exhibited properties of a catch bond, with the lifetime increasing tenfold when the pulling force increased from 10 to 20 pN. We also show that silica beads were more appropriate than polystyrene beads for the force measurements, as tethers, longer than 200 nm, could be extracted from polystyrene beads.

S Online supplementary data available from stacks.iop.org/Nano/21/255102/mmedia

1. Introduction

A major challenge in molecular and cellular biology is to investigate biological processes under physiological conditions. Many of these processes occur within the confines of cellular compartments and/or the surfaces of lipid membranes. Therefore, the working area per volume has a length scale of less than 100 nm and involves tens of molecules. In many cases, studies need to be carried out with individual cells, since it is impossible to mimic the conditions of the cellular environment *in vitro*. A technique that was designed to meet these challenges is the photonic force microscope (PFM) [1, 2]. This approach builds on advances of laser trap technology [3–5] and ultrafast sub-nanometer resolution particle detection to probe the local environment of the trapped particle in three dimensions (3D) [6]. The optical forces generated by a PFM on a small particle, acting as a force sensor, are typically in the piconewton range, making it an ideal tool for studying the mechanics of individual molecules such as kinesin [7, 8] and myosin [9]. The PFM is also ultrasensitive to the local environment under investigation. Using the PFM, Pralle *et al* measured the size of protein lipid rafts by recording the diffusion of a microsphere specifically coupled to the membrane of a living cell [10]. The PFM has also been employed as a high resolution device to image the 3D volume of a polymer network [11].

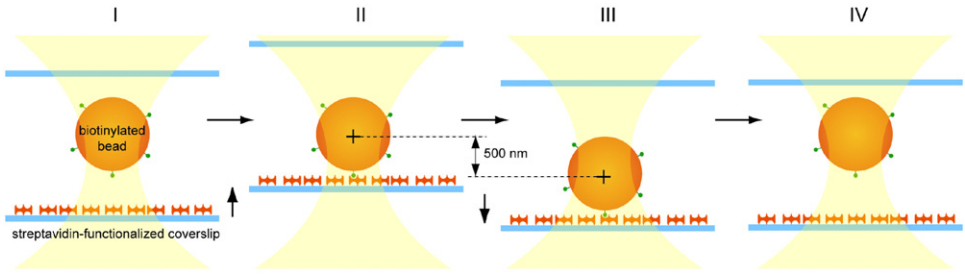

Figure 1. Schematics of biotin–streptavidin binding measurements. The automated experimental protocol can be divided into four steps: (I) approach of the bead to the surface, (II) binding, (III) pulling, and (IV) unbinding. It should be noted that the absolute position of the optical trap remained stationary. The relative position of the bead to the streptavidin-coated coverslip was adjusted during the measurement by changing the position of the coverslip via a piezoelectric stage.

(This figure is in colour only in the electronic version)

More recently, the PFM was applied to measure nanoscale surface forces and friction at a plane surface [12], to track the 3D dynamics of macrophage membrane protrusions during phagocytosis [13], to detect sequential bond formation between a biotin–streptavidin ligand–receptor pair [14], and to assess protein friction between a single kinesin motor molecule and its underlying microtubule [15].

In the current report, we describe the development of an approach based on the PFM that automated and greatly accelerated the acquisition of force measurements of ligand–receptor interaction. The experimental principle of our PFM force-dependent kinetic measurement is illustrated in figure 1. A receptor-functionalized coverslip was lightly pressed against an optically trapped ligand-functionalized microbead to facilitate the formation of a ligand–receptor complex. To dislodge the bound bead from the surface, the trapping potential was strengthened by increasing the output power of the trapping laser. Subsequent lowering of the coverslip displaced the bead from the trap center and generated a vertical pulling force on the bead. The bead remained attached to the surface until the ligand–receptor complex ruptured. The survival time of the complex depended on the intrinsic properties of ligand–receptor interaction and the number of ligand–receptor bonds formed.

For this study, we used the biotin–streptavidin complex as a model system for ligand–receptor interactions [16, 17]. Streptavidin is a 52.8 kD protein isolated from the bacterium *Streptomyces avidinii*. Its active form is a tetramer, capable of binding four biotins, a B-complex vitamin involved in the metabolism of fatty acids and amino acids. The streptavidin–biotin complex is extremely stable over a range of temperature and pH and is a model system for high affinity interaction. The biotin–streptavidin system has been extensively characterized, including by direct force measurements [18–26].

2. Methods and materials

2.1. Functionalized beads and coverslips

One micrometer sized silica beads (SS04N/9189; Bangs Laboratories, Inc., Fishers, IN) were derivatized with biotin according to Steinberg *et al* [27]. Silica beads, activated by 3-aminopropyltrimethoxysilane, were functionalized with NHS-PEG4-biotin (Pierce, Rockford, IL). Biotinylated 1.75 μm sized polystyrene beads were also purchased from Bangs Laboratories (CP10F/8575: 1.75 μm Dragon Green (480, 520) fluorescent, biotin-coated polystyrene, 1% solids, binding capacity $= 0.07$ μmol biotin mg^{-1}) and used without further modification. The choice of the bead size for each bead material (silica or polystyrene) was motivated by the extent of optical forces generated by the laser trap when interacting with the bead. In order to generate sufficient force to rupture the intermolecular bonds that stabilize a streptavidin–biotin complex, a high vertical trapping force constant, k_Z, is needed. This is achieved for bead sizes close to the wavelength, $\sim$1 μm, of the trapping laser [28]. In general, due to their lower refractive index, silica beads generate lower forces than polystyrene beads. Therefore, for comparison, we chose the polystyrene to have a bead size allowing for comparable trapping forces to a 1 μm silica bead. The trapping force constants, k_X, k_Y, k_Z, were determined in 3D for both bead types used experimentally through the PFM calibration procedure described below.

To immobilize streptavidin on glass coverslips, a stock solution of streptavidin (Thermo Fisher Scientific, Switzerland) at 5 mg ml^{-1} was prepared in 100 mM $NaHCO_3$, pH 9. 50 μl spots of streptavidin at different concentrations were adsorbed on the coverslip overnight (12 h for consistency) at 4 °C, and then blocked with 1% BSA in 100 mM $NaHCO_3$, pH 9 for 2 h at room temperature.

2.2. Photonic force microscope

A detailed description of our PFM setup is given in the supplementary data (available at stacks.iop.org/Nano/21/255102/mmedia).

2.3. Calibration of PFM

Calibration consists in determining the position calibration factor β and the spring constant k of the optical trapping potential for all three axes, X, Y and Z. The axial (along Z) position fluctuations of the trapped bead are measured by the intensity ratio of the scattered laser light to the total amount

of light reaching the detector [6]. β for each dimension is given in units of nm V^{-1} since the acquired position signal is recorded in volts, and the position of the particle is expressed in nanometers. For PFM calibration, we use the method developed by Tolić-Nørrelykke *et al* [29]. A defined fluid flow around the bead was created by moving the whole sample chamber through the piezo scanning table with a sinusoidal oscillation $x_{\rm drive}(t) = A\sin(2\pi f_{\rm drive}t)$ at a given amplitude $A = 100$ nm and frequency $f_{\rm drive} = 10$ Hz, while the laser trap remains fixed. The sphere was typically positioned at a distance $h = 10R_{\rm bead}$ from the glass surface to avoid any boundary effects [30]. The resulting power spectral density $P(f)$ for long measurement times of typically 50 s is given by

$$P(f) = P_{\rm therm}(f) + P_{\rm drive}(f) = \frac{D}{\pi^2\left(f^2 + f_{\rm c}^2\right)} + \frac{A^2}{2(1 + f_{\rm c}^2/f_{\rm drive}^2)}\delta(f - f_{\rm drive}), \quad (1)$$

where D is the diffusion coefficient given by Einstein's relation $D = k_{\rm B}T/6\pi\eta R_{\rm bead}$ and $f_{\rm c}$ the corner frequency. Equation (1) is the superposition of the 'thermal background' arising from Brownian fluctuations ($P_{\rm therm}(f)$, first term) with a delta function spike at the driving frequency of the stage ($P_{\rm drive}(f)$, second term). This 10 Hz peak appears only in the power spectral density measured along the oscillation direction X (figure 2(A)), if the PFM is well aligned (see section 2.4). With bead sizes and the trapping stiffness used here, hydrodynamic effects arising from the fluid and particle inertia can be neglected [31]. The experimentally measured $P_{\rm drive}^{\rm exp}(f)$ is expressed in V^2 Hz^{-1} and is related to $P_{\rm drive}(f)$ through the relation giving us β:

$$P_{\rm drive}(f) = \beta^2 P_{\rm drive}^{\rm exp}(f) \quad (2)$$

$P_{\rm drive}(f)$ is known from equation (1), since A and $f_{\rm drive}$ are known *a priori* and $f_{\rm c}$ is known experimentally. Equivalently the diffusion coefficient $D^{\rm exp}$ is measured in V^2s and given by $D = \beta^2 D^{\rm exp}$. The trapping stiffness k is then determined through $f_{\rm c}$ and $D^{\rm exp}$ for all three dimensions:

$$k = 2\pi f_{\rm c}\frac{k_{\rm B}T}{\beta^2 D^{\rm exp}}. \quad (3)$$

With this method, the quantitative characterization around Brownian motion requires knowledge of the local temperature of the bead. Temperature variations arise from laser-induced heating and affect the viscosity of the surrounding fluid [32, 33]. For the experiments performed by using low laser powers, i.e. low trap stiffnesses, no significant temperature increase was observed. In contrast, laser-induced heating became critical at high trapping forces, when maximal laser powers were employed to disrupt the ligand–receptor bond. In order to check for possible temperature changes in the laser focus, we first determined the aqueous medium's viscosity from

$$\eta = \frac{k_{\rm B}T[P(f_{\rm drive}) - P_{\rm therm}(f_{\rm drive})]}{3\pi^3 a A^2 f_{\rm drive}^2 P(f_{\rm drive}) t_{msr}} \quad (4)$$

and then looked for the temperature corresponding to such a water viscosity. The newly defined temperature, which was typically around 28 °C, was then used for determination of β.

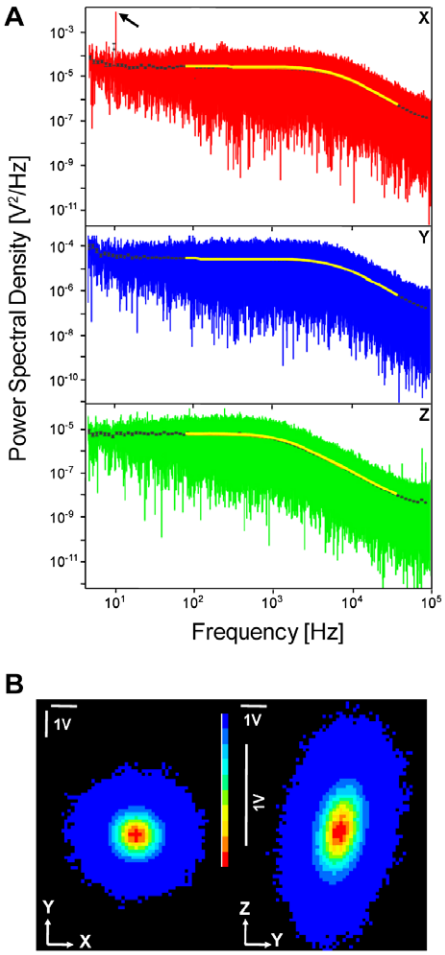

Figure 2. 3D calibration and alignment of the laser trap holding a 1 μm sized biotinylated silica bead at ~10 μm away from the streptavidin-coated surface. (A) Log–log plot of the corresponding raw power spectral density $P(f)$ calculated from the position fluctuations in X, Y, and Z directions (red, blue, and green lines, respectively), blocked in 20 bins/decade (black dotted line) and fitted by the first term of equation (1) (yellow line). The black arrow in the X graph indicates the peak at the driving frequency of the oscillatory flow, arising from the Stokes drag. The sampling frequency was 200 kHz and the measurement time was 50 s. The position calibration factors in each dimension were $\beta_X = 10$ nm V^{-1}, $\beta_Y = 9$ nm V^{-1}, $\beta_Z = 84$ nm V^{-1}, and the trap stiffnesses were $k_X = 206$ μN m^{-1}; $k_Y = 217$ μN m^{-1}; $k_Z = 52$ μN m^{-1}. (B) 2D histogram of the bead center positions. The XY histogram reflects the lateral movement of the trapped bead, showing the expected symmetry. The YZ histogram highlights a small tilt with respect to the optical axis, which can be further corrected by realigning the OBJ, CND, and QPD.

2.4. Alignment of PFM

The objective, condenser and QPD have to be precisely aligned along the optical axis defined by the laser beam path, in order to optimize sensitivity and reduce cross-talk between the axial (Z) and the lateral (X and Y) channels of the QPD. Cross-talk may lead to underestimates of the trapping stiffness [29] as well as to distortions in the symmetry of the 3D trapping potential. Therefore, the QPD, CND and OBJ were repositioned relative to the laser beam axis, while monitoring online the 2D projections of the trapped particle's position

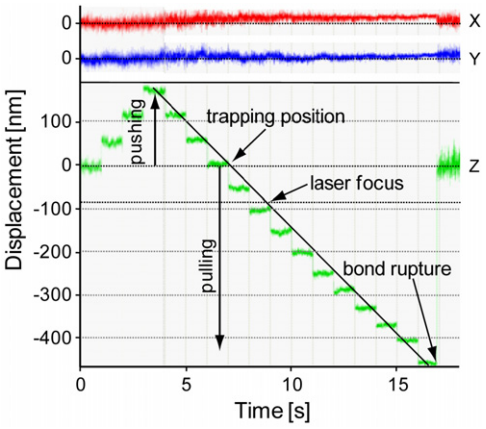

Figure 3. Detector linearity. Time traces in X (red), Y (blue) and Z (green) directions as a biotin bead bound to the streptavidin surface was pushed out of its trapping position by the piezo stage in three steps of 50 nm, and then pulled back for ∼500 nm until the bond ruptured. The black diagonal line is a guide to the eye and indicates that our PFM system was linear in a range between +200 and −200 nm from the focus.

histograms (figure 2(B)). The PFM is considered as well aligned when the histograms along X and Y are symmetric, and the direction along Z is close to vertical, i.e. perpendicular to the focal plane. A further check for cross-talk is the absence of the 10 Hz peak in the power spectral density of the Y and Z (figure 2(A)).

2.5. PFM linearity

In our experiments the bead bound to the coverslip via a biotin–avidin bond is offset by typically 300–500 nm from its trapping position, once the coverslip is pulled away (figure 1). As PFM linearity depends on the bead size and material, we determined the linearity range of the PFM system for each bead type used. The equilibrium position of a 1 μm silica bead inside the optical trap relative to the laser focus was measured to be ∼90 nm as described in [34]. The position of the streptavidin-coated coverslip relative to the focus of the optical trap was regulated by the piezoelectric stage. Upward displacement of the coverslip at 50 nm increments along the optical z axis was used to push the coverslip against the bead (figure 3), allowing the streptavidin–biotin bond to be formed. The motion of the piezo stage was then reversed, and the bound bead was pulled back, again in 50 nm steps, through its trapping position, past the laser focus, until the bond ruptured at an offset of ∼500 nm. The black diagonal line in figure 3 highlights deviations from the linear regime of the detection system. This procedure also represents a cross-check of the accuracy of the determination of β along Z, where the bead positions relative to the trapping position can be directly compared to the 50 nm steps performed by the piezo stage along Z, calibrated by the manufacturer.

3. Results

3.1. Description of the experimental system

As a model system to study the effect of pulling force generated by the PFM on the unbinding of a ligand–receptor complex, we investigated the interaction of a biotin-functionalized bead with a coverslip surface coated with streptavidin by PFM force measurement. The experimental design of these measurements is illustrated in figure 1. One micrometer silica microbeads, lightly functionalized with biotin, were injected into a sample chamber formed by a microscope slide and a glass coverslip functionalized with streptavidin. When the coverslip was coated with streptavidin at 0.5 mg ml^{-1}, many of the beads remained in suspension for an extended period of time (>2 h). The suspended beads were distinguishable from the bound beads since they were out of focus and diffused randomly. A selected bead was identified and positioned close to the optical trap. Once trapped, the bead was confined to a small volume, about a hundred nanometers above the focus of the optical trap of the PFM (step I of figure 1). The amplitude of the bead's position distribution was determined by the strength of the trapping potential [28, 29]. In order for the bead to be more sensitive to local force changes upon binding, a weak trapping potential was used at this point in the measurement. This conferred to the bead greater freedom to explore potential binding sites. When the streptavidin-coated coverslip was elevated, bringing the coverslip closer to the trapped bead and eventually making contact with the biotin bead, its movement was further restricted, first by the surface and then, even more, when it was bound to streptavidin (step II of figure 1). To dislodge the bound bead from the surface, the streptavidin-coated coverslip was lowered, resulting in a displacement of the bead relative to the trapping potential of the PFM and a vertical pulling force on the bead. The bead remained attached to the surface until the biotin–streptavidin complex(es) ruptured. Breakage of the biotin–streptavidin bond(s) was characterized by the sudden return of the bead to its equilibrium position in the trap and an increase of its fluctuation volume. The survival time of the complex depended on the strength of the pulling force and is an intrinsic property of the biotin–streptavidin complex.

Figure 4(A) presents the time trace of a bead's thermal position fluctuations in an optical trap in close proximity to a streptavidin-functionalized surface, but initially not immobilized via streptavidin–biotin bonds. As shown, seven sections of the time trace, labeled a–g, were selected for analysis. Figure 4(B) presents the corresponding 2D position histograms (top XZ; middle YZ; bottom XY) of the bead. The isosurface of the 3D position histogram (not shown) resembles a prolate spheroid with elongation along the Z axis. At section a, the biotinylated bead was approximately 10 nm above the streptavidin-functionalized coverslip. Spatial fluctuations were approximately 150 nm along the X and Y axes parallel to the plane of the coverslip and about 300 nm along the axis (Z) perpendicular to the coverslip. The 2D histogram of section a along the XY plane was radially symmetrical. The asymmetry observed in both XZ and YZ histograms can be attributed to the close proximity of the bead to the coverslip, which restricted the displacement of the bead. Between sections a and b the coverslip was elevated 50 nm towards the trapped bead, further restricting the fluctuation of the bead along the Z axis. In section c, the bead experienced a sudden change in spatial fluctuations that was most pronounced along the X and

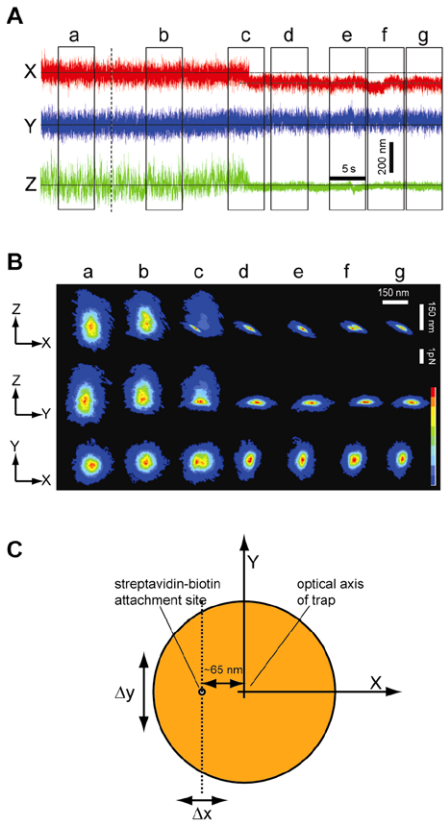

Figure 4. Detection of single molecule binding by PFM. (A) Time traces of position fluctuations along the X (red), Y (blue), and Z (green) axes of a biotin bead held by a weak optical trap ($k_X = 4.3\ \mu\text{N m}^{-1}$; $k_Y = 4.5\ \mu\text{N m}^{-1}$; $k_Z = 1.6\ \mu\text{N m}^{-1}$) in close proximity to a streptavidin-coated coverslip. Sections a–g were selected for analysis. (B) 2D histograms of the bead in the X–Z, Y–Z, and X–Y planes for sections a–g of the time trace. Changes in thermal position fluctuations along the X, Y, and Z axes during the course of bead–coverslip interaction and eventual receptor–ligand binding are clearly visible. (C) Model for the thermal fluctuation of a bead that is attached to a point along the X axis away from the center of the optical trapping axis.

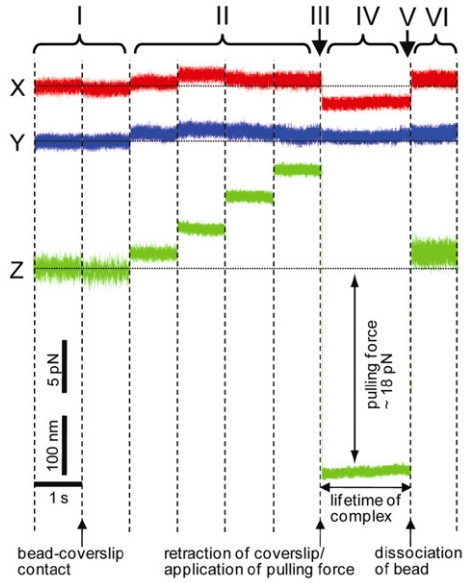

Figure 5. Pulling force accelerated the dissociation of the streptavidin–biotin complex. 3D time trace records of the position fluctuation of the biotin bead during a PFM force measurement. In region I, the bead was close above the streptavidin-functionalized coverslip. In region II the coverslip was pressed against the bead. At III lowering the coverslip pulled the bead away from the center of the optical trap. In V dissociation of the streptavidin–biotin bond returned the bead to its original position ($k_X = 202\ \mu\text{N m}^{-1}$; $k_Y = 221\ \mu\text{N m}^{-1}$; $k_Z = 56\ \mu\text{N m}^{-1}$).

Z axes. Moreover, its fluctuations in Z revealed a downward displacement (∼60 nm) of the bead towards the coverslip that was consistent with binding of the bead to the coverslip. Interestingly, this binding event resulted in a bead displacement also along the X axis, but not the Y axis, relative to the beam axis of the optical trap. We interpreted these observations to correspond to the formation of a streptavidin–biotin bond along the X axis (see figure 4(C)). As a consequence of both the formation of the streptavidin–biotin bond and the off-centered position of the bond relative to the optical axis of the trap, there was a significant reduction in the magnitude of X fluctuations. There was some reduction in fluctuations along the Y direction, but not as significant. In sections d–g of the time trace, the bead was bound to the surface of the coverslip via a single streptavidin–biotin linkage. The 2D histograms revealed that formation of the streptavidin–biotin bond restricted the movement of the bead mainly along the vertical axis. The lateral movement of the bead was less restricted, as the bead was able to pivot about its attachment point. Figure 4(C) presents a schematic illustration of the trapped bead bound to the surface via a streptavidin–biotin bond that is consistent with the recorded time trace. The tilt observed in the XZ histograms derived from sections d–g provided additional support to the assertion that the streptavidin–biotin attachment point was offset along the X axis.

3.2. Force-dependence of dissociation of the biotin–streptavidin bond

The PFM was used to determine how a pulling force affected the survival time of the biotin–streptavidin bond. A typical set of recordings from these experiments is presented in figure 5. In order to generate sufficient force to induce the dissociation of the streptavidin–biotin linkage, the trapping potential was strengthened by a factor of 35 by increasing the incoming power of the IR laser. As a consequence, the thermal fluctuations of the trapped bead (figure 5, region I) were significantly reduced compared to the weakly trapped bead of figure 4. Hence, relative changes of the position fluctuations due to additional confinement became less visible. To identify the point of bead–coverslip contact, the coverslip was elevated in 50 nm steps until it displaced the bead out of its trapping position, as detected in the Z-axis time trace. Since the amplitude of the position fluctuations of the suspended bead was ∼30 nm in Z, a displacement of 50 nm was readily detected (figure 5, region II). This, along with the delay in region II, determined the number of streptavidin–biotin bonds formed between the bead and the coverslip. To disrupt the

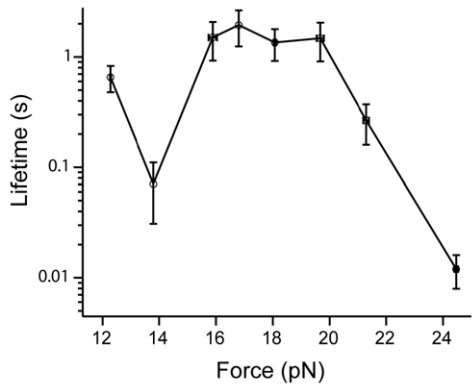

Figure 6. Lifetime of streptavidin–biotin bond as a function of pulling force. The error bars correspond to the standard error of the mean.

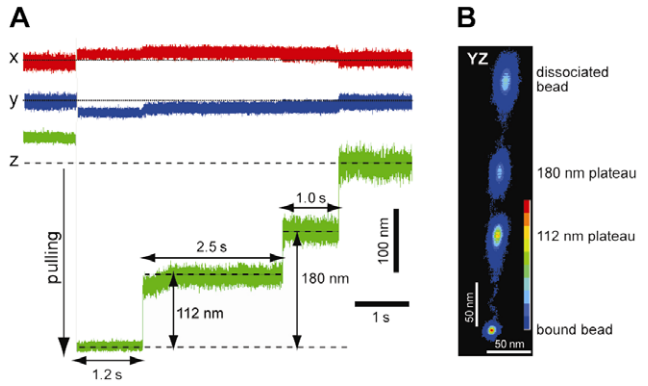

Figure 7. Extension of a polymer tether from a PS bead during force measurements. (A) Time trace records of the position fluctuation of the biotin-labeled PS bead during a PFM force measurement. (B) 2D histograms of the bead's positions in the X–Z and Y–Z planes highlighting the position distributions at each plateau. The XY histogram points to a slight offset between the tether and optical axis.

streptavidin–biotin linkage, the coverslip was lowered, pulling the attached bead with it (figure 5, III). As a first order approximation, the trapping potential of the PFM can be considered as a harmonic potential. A vertical displacement Z of the bead away from its equilibrium position resulted in a restoring force F_Z that pulled the bead away from the coverslip (figure 5, region IV). Eventually, the upward pulling force on the bead broke the streptavidin–biotin linkage (figure 5, V). The unbinding of the streptavidin–biotin complex was detected as a sudden displacement of the bead in the Z direction, back to its original equilibrium position. The severed linkage also permitted the bead to fluctuate again within the confines of the optical trap alone (figure 5, region VI).

The lifetime of the streptavidin–biotin complex in the presence of a pulling force was given by the duration of region IV in figure 5. As summarized in figure 6, the lifetime of the streptavidin–biotin complex depended on the pulling force of the optical trap. Interestingly, our measurements revealed that there was an increase in complex lifetime from 14 to 17 pN, then a plateau to 20 pN before decaying exponentially toward zero at higher forces. The exponential dependence in the force regime above 20 pN is consistent with the standard Bell model [35]. Overall, the observed properties of the streptavidin–biotin interaction are characteristics of a catch bond that have been detected in other ligand–receptor systems [36–39].

3.3. Forced extension of polymer in polystyrene bead tethers

As polystyrene (PS) beads are typically used in single molecule optical trap measurements, we performed the same experiments as above with 1.75 μm PS beads. The PS beads have the advantage that they can generate higher forces than silica beads due to their refractive index. PS is also favored because the local temperature of the trapped bead is not elevated as much as is the case for silica beads. To make biotin-coated spheres, a biotin derivative is conjugated to carboxylate-modified polystyrene spheres. The hydrophilic carboxylic acid-containing monomers used to modify the PS bead can polymerize at the bead surface to form loosely associated water-soluble polymer (WSP) chains. Most of the loosely bound WSP is washed away after polymerization, but permanently bound WSP chains may be available for biotin immobilization. Our PFM binding measurements revealed that the polymer tethers can extend over 200 nm away from the surface. In the measurement presented in figure 7, a biotin-functionalized PS bead, bound to a streptavidin-coated coverslip, was displaced by a distance of about 300 nm away from the center of the optical trap, generating a pulling force of about 17 pN between the bead and coverslip. After about 1.2 s, the bead suddenly displaced 112 nm toward center of the trap. An increase in the thermal position fluctuations of the bead further supported the interpretation that the bead moved away from the surface of the coverslip. The bead remained at this position for about 2.5 s before it displaced again to a height of 180 nm above the coverslip, but not free of the coverslip. It remained at this position for 1 s before displacing to the center of the trap. The 2D position histograms show only a slight confinement of the bead by the PS tether along all three dimensions, indicating that the tether is only slightly stiffer than the optical trap with $k_X = 202\ \mu\text{N m}^{-1}$; $k_Y = 221\ \mu\text{N m}^{-1}$; and $k_Z = 56\ \mu\text{N m}^{-1}$ (figure 7(B)). The XY position histograms revealed a slight offset between the tether axis and the optical trap axis along both directions X and Y. The presence of the two plateaus at 112 and 180 nm can be interpreted as successive extraction of a WSP chain from the PS bead, as no such plateaus were detected in measurements carried out with silica beads. The extension of the WSP appeared to be force dependent. At low force, the frequency of WSP extension was low. At ~20 pN, 30% of the measurements revealed polymer extension with an average extension length of ~200 nm.

4. Discussion and conclusion

Optical trap experiments provide detailed dynamic information on an individual molecule and its surroundings. Although it is a powerful technique, it is still the domain of specialists.

This is not only because precise alignment of the instrument is required, but also because the measurements themselves are challenging and tedious. To take advantage of the greater lateral (X or Y) force generated by an optical trap, most commonly used experimental designs use two beads; one stationary and the second manipulated by the optical trap along the X or Y axis towards the stationary bead [40]. When both beads are brought into close contact with each other for interaction, scattering of the trapping laser will occur, degrading the signal-to-noise ratio and making it more difficult to estimate the force on the trapped bead [30]. To avoid this drawback, the two beads are often linked in a so-called dual-trap dumbbell assay via a long DNA tether that is difficult to visualize and hence to control the second bead. The vertical force generated by an optical trap is typically three to five times weaker than the force generated laterally. However, by optimizing the alignment and selecting the appropriate bead size, we were able generate an optical trap that can exert a vertical pulling force in excess of 50 pN. These forces allowed us to reduce the survival time of the high affinity streptavidin–biotin complex to subseconds from hours, and should be sufficient to rupture most biomolecular interactions of interest in the time regime of seconds or less.

A strong vertical force allowed us to develop a semi-automated system for the acquisition of force-dependent kinetic measurements using the PFM. This was possible due to the configuration of our experimental system. The biotin beads were inserted between two glass coverslips that formed the sample chamber. Unbound beads were readily distinguished from beads bound to the streptavidin-coated coverslip by their diffusive motion. Our control system allowed us to select a bead from view, capture it with the optical trap, and perform the force measurement. The sample chamber was fixed on a computer controlled 3D piezo scanning stage. The motion of the scanning stage was automated in order to allow a reproducible approach and retraction of the coverslip, functionalized with streptavidin, towards the trapped biotinylated bead. Our system also semi-automatically calibrated the trapping potential and determined if the bead was coupled to the coverslip by one or multiple bonds. As a result, hundreds of measurements were acquired in one session.

An important feature of our PFM system is its ability to distinguish between the formation of one and multiple bonds in our measurements prior to the application of a pulling force. The number of biotin–streptavidin bonds formed depended on a number of factors including the surface density of both streptavidin and biotin, the duration of biotin bead–streptavidin coverslip contact and how hard the bead was pressed against the coverslip. To identify conditions for single streptavidin–biotin bond formation, biotin beads were prepared at different amounts of labeled biotin. Conditions were worked out so that the binding between a biotin bead and the streptavidin coverslip occurred at a frequency of about 10% following bead–coverslip contact. Under these conditions, the probability that the detected adhesion event is mediated by a single streptavidin–biotin bond is approximately 0.95 [41]. Bond formation was accompanied by a reduction of the vertical fluctuation and a lateral displacement of the bead as shown in figure 4. In most cases, there was no further change in the 2D histograms after the initial bond is formed on the timescale of 10 s, indicating that no second bond formed. The formation of multiple bonds will further restrict the fluctuations of the bead and break the radial symmetry of the XY 2D histogram as reported by Bartsch *et al* [14].

Our analysis of the PFM measurements revealed that the streptavidin–biotin interaction deviated from the standard Bell model [39] at pulling forces less than 20 pN, and exhibited properties of a catch bond. Although the streptavidin–biotin interaction has been extensively studied by other direct force spectroscopy techniques, including AFM and biomembrane probes [18–21], its catch-bond-like characteristics have not yet been reported. However, it should be noted that catch-bond-like properties are not directly evident in the force ramp methods used in the previous studies. Although the catch bonds represent counterintuitive behaviors, they are not uncommon. Using force clamp techniques similar to the approach employed in the current work, a number of ligand–receptor systems have been shown to form catch bonds. Specifically, catch bonds have been demonstrated in interactions between selectins and ligands [36], actin and myosin [37], FimH receptor and mannose [38], and fibronectin and the $\alpha_5\beta_1$ integrin [39]. Their unusual properties have been attributed to a force-induced structural/conformational change in the binding site of the interacting molecules.

In summary, we have developed a method to study the effects of an applied force on biomolecular bonds by PFM. The accessible forces range from a fraction of 1 pN to 50 pN and are ideally suited for ligand–receptor studies. Our experimental design can be readily adapted to studies involving live cells. This opens up the possibility of studies on the regulatory role of the cell in processes such as cell adhesion and migration. In this process the pulling force is not necessarily perpendicular to the membrane. Our 3D experimental setup will allow us to probe the effect of a pulling force in any arbitrary direction. Such studies are expected to reveal greater insights into biological processes.

Acknowledgments

This work was supported by grants from the Swiss National Science Foundation (SNF) through the R'Equip project No 206021_121396 for equipment, the SNF-NCCR-Nano and the M E Müller Foundation of Switzerland to SJ, the NCCBI to FM, the University of Applied Sciences of Western Switzerland (HEIG-VD) to RK, and the NIH (GM086808) to VTM.

References

[1] Ghislain L P and Webb W W 1993 *Opt. Lett.* **18** 1678
[2] Florin E L, Pralle A, Horber J K and Stelzer E H 1997 *J. Struct. Biol.* **119** 202–11
[3] Ashkin A and Dziedzic J M 1987 *Science* **235** 1517–20
[4] Neuman K C and Block S M 2004 *Rev. Sci. Instrum.* **75** 2787–809

[5] Moffitt J R, Chemla Y R, Smith S B and Bustamante C 2008 *Annu. Rev. Biochem.* **77** 205–28
[6] Pralle A, Prummer M, Florin E L, Stelzer E H and Horber J K 1999 *Microsc. Res. Tech.* **44** 378–86
[7] Kuo S C and Sheetz M P 1993 *Science* **260** 232–4
[8] Jeney S, Stelzer E H K, Grubmuller H and Florin E L 2004 *ChemPhysChem* **5** 1150–8
[9] Molloy J E, Burns J E, Kendrick-Jones J, Tregear R T and White D C S 1995 *Nature* **378** 209–12
[10] Pralle A, Keller P, Florin E L, Simons K and Horber J K 2000 *J. Cell Biol.* **148** 997–1008
[11] Tischer C, Altmann S, Fisinger S, Stelzer E H K, Hörber J K H and Florin E L 2001 *Appl. Phys. Lett.* **79** 3878–80
[12] Schaffer E, Norrelykke S F and Howard J 2007 *Langmuir* **23** 3654–65
[13] Kress H, Stelzer E H, Holzer D, Buss F, Griffiths G and Rohrbach A 2007 *Proc. Natl Acad. Sci. USA* **104** 11633–8
[14] Bartsch T F, Fisinger S, Kochanczyk M D, Huang R, Jonas A and Florin E L 2009 *ChemPhysChem* **10** 1541–7
[15] Bormuth V, Varga V, Howard J and Schaffer E 2009 *Science* **325** 870–3
[16] Green N M 1990 *Methods Enzymol.* **184** 51–67
[17] Laitinen O H, Hytonen V P, Nordlund H R and Kulomaa M S 2006 *Cell. Mol. Life Sci.* **63** 2992–3017
[18] Lee G U, Kidwell D A and Colton R J 1994 *Langmuir* **10** 354–61
[19] Florin E L, Moy V T and Gaub H E 1994 *Science* **264** 415–7
[20] Merkel R, Nassoy P, Leung A, Ritchie K and Evans E 1999 *Nature* **397** 50–3
[21] Rico F and Moy V T 2007 *J. Mol. Recognit.* **20** 495–501
[22] Leckband D, Müller W, Schmitt F-J and Ringsdorf H 1995 *Biophys. J.* **69** 1162–9
[23] Breisch S, Gonska J, Deissler H and Stelzle M 2005 *Biophys. J.* **89** L19–21
[24] Reichle C, Sparbier K, Müller T, Schnelle T, Walden P and Fuhr G 2001 *Electrophoresis* **22** 272–82
[25] Pierrat S, Brochard-Wyart F and Nassoy P 2004 *Biophys. J.* **87** 2855–69
[26] Pincet F and Julien Husson J 2005 *Biophys. J.* **89** 4374–81
[27] Steinberg G, Stromsborg K, Thomas L, Barker D and Zhao C 2004 *Biopolymers* **73** 597–605
[28] Rohrbach A 2005 *Phys. Rev. Lett.* **95** 168102
[29] Tolić-Nørrelykke S F, Schäffer E, Howard J, Pavone F, Jülicher F and Flyvbjerg H 2006 *Rev. Sci. Instrum.* **77** 103101
[30] Jeney S, Lukić B, Kraus J A, Franosch T and Forró L 2008 *Phys. Rev. Lett.* **100** 240604
[31] Lukic B, Jeney S, Sviben Z, Kulik A J, Florin E L and Forro L 2007 *Phys. Rev.* E **76** 011112
[32] Guzmán C, Köszali R, Mor F, Ecoffet C, Flyvbjerg H, Forró L and Jeney S 2008 *Appl. Phys. Lett.* **93** 184102
[33] Peterman E J, Gittes F and Schmidt C F 2003 *Biophys. J.* **84** 1308–16
[34] Lang M J, Asbury C L, Shaevitz J W and Block S M 2002 *Biophys. J.* **83** 491–501
[35] Bell G I 1978 *Science* **200** 618–27
[36] Marshall B T, Long M, Piper J W, Yago T, McEver R P and Zhu C 2003 *Nature* **423** 190–3
[37] Guo B and Guilford W H 2006 *Proc. Natl Acad. Sci. USA* **103** 9844–9
[38] Yakovenko O, Sharma S, Forero M, Tchesnokova V, Aprikian P, Kidd B, Mach A, Vogel V, Sokurenko E and Thomas W E 2008 *J. Biol. Chem.* **283** 11596–605
[39] Kong F, Garcia A J, Mould A P, Humphries M J and Zhu C 2009 *J. Cell Biol.* **185** 1275–84
[40] Bianco P, Nagy A, Kengyel A, Szatmári D, Mártonfalvi Z, Huber T and Kellermayer M S Z 2007 *Biophys. J.* **93** 2102–9
[41] Tees D F J, Waugh R E and Hammer D A 2001 *Biophys. J.* **80** 668–82